Available online at www.sciencedirect.com
ScienceDirect
Scripta Materialia 57 (2007) 747–750
Scripta MATERIALIA
www.elsevier.com/locate/scriptamat

Controlled formation of nanoscale wrinkling patterns on polymers using focused ion beam

Myoung-Woon Moon,[a] Sang Hoon Lee,[b] Jeong-Yun Sun,[b] Kyu Hwan Oh,[b] Ashkan Vaziri[a] and John W. Hutchinson[a,*]

[a] *School of Engineering and Applied Sciences, Harvard University, 29 Oxford Street, Cambridge, MA 02138, USA*
[b] *Department of Materials Science and Engineering, Seoul National University, San 56-1 Shillim, Kwanak, Seoul 151-744, Republic of Korea*

Received 11 May 2007; revised 31 May 2007; accepted 16 June 2007
Available online 23 July 2007

It has previously been shown that focused ion beam irradiation induces a wrinkled skin on the surface of polydimethylsiloxane. Here, it is demonstrated that the wavelength of the induced wrinkles and their morphology can be effectively selected by controlling the acceleration voltage and fluence of the ion beam. The capabilities of the technique are also extended by adopting the maskless patterning method of the focused ion beam system, which allows creation of controlled wrinkling patterns on small surfaces of polymers.

Keywords: Focused ion beam; Surface modification; Polydimethylsiloxane; Wrinkles; Maskless patterning method

Modification of the surface of polymers at the micron and submicron scales has direct implications for an array of scientific and technological areas from tissue engineering to building high-capacity memory storage devices [1–5]. In tissue engineering, for example, certain aspects of cell behavior can be controlled by altering surface topology [6–10]. Other potential applications include optical diffraction gratings and optical microlenses [11,12], biosensors [13,14], and microfluidic devices [15–18]. Recently, we have shown that irradiation of Ga^+ focused ion beam (FIB) on the surface of a polydimethylsiloxane (PDMS) substrate (Fig. 1a) results in the formation of a stiff skin on the substrate, which has a chemical composition resembling amorphous silica [1]. This stiff skin undergoes ion-irradiation-induced anisotropic plastic deformation and tends to expand in the plane perpendicular to the ion beam [19–23]. Since the stiff skin deformation is constrained by the PDMS substrate, the skin experiences in-plane compressive strain upon ion beam irradiation and buckles to accommodate the induced mismatch strain between the skin and the polymeric substrate. This finding provides a robust technique for creating wrinkling patterns on selective areas of the PDMS by simply controlling the movement of the ion beam relative to the polymeric substrate. A Ga^+ ion beam with acceleration voltage of 30 keV and ion fluence in the range of 10^{12}–10^{16} ions cm^{-2} produces a variety of wrinkling patterns with primary wavelength ~450 nm, from straight one-dimensional undulations to herringbone and hierarchical patterns with multiple wavelength scales [1]. In this paper, the roles of the acceleration voltage and the fluence of the ion beam are explored by systematically varying these parameters over the range 5–30 keV and 10^{12}–10^{18} ions cm^{-2}, respectively.

PDMS networks were prepared by a mixture of elastomer and cross-linker in a mass ratio of 10:1 (Sylgard-184, Dow Corning, MI). The mixture was placed in a plastic box and stirred to remove trapped air bubbles and then cured at 80 °C for 2 h, resulting in a cross-linked PDMS network with elastic modulus ~2 MPa [24]. PDMS coupons of dimension 20 mm × 20 mm × 3 mm were cut for the experiments. A high-resolution field emission scanning electron microscopy (FESEM)/FIB dual beam system (FE-SEM/FIB Dual Beam NOVA, FEI, OR) was employed for focused ion beam irradiation and SEM imaging. PDMS coupons were placed in the high-vacuum chamber under a working pressure of $\sim 5 \times 10^{-5}$ Pa. The PDMS surface was

* Corresponding author. E-mail: jhutchin@fas.harvard.edu

1359-6462/$ - see front matter
doi:10.1016/j.scriptamat.2007.06.043

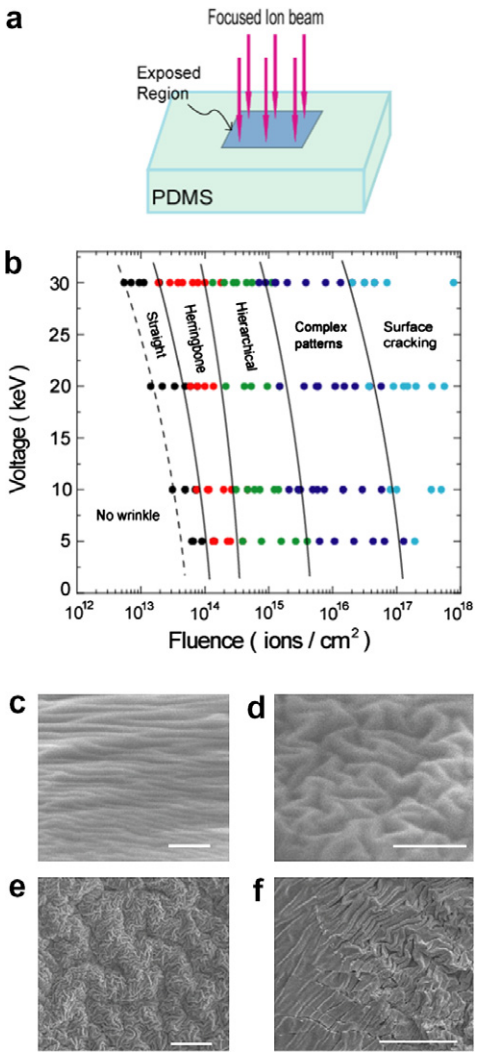

Figure 1. Morphology of the wrinkling patterns created by varying the ion beam acceleration voltage and fluence. (a) A schematic of the experiment. Wrinkles appear only on the areas of the PDMS exposed to FIB. (b) Map of wrinkle morphology as a function of FIB acceleration voltage and ion beam fluence. The wrinkling patterns were classified in five different categories: straight, herringbone, hierarchical, complex patterns and surface cracking. The filled circles show the actual data for the morphology of the created wrinkles. (c–f) Selected SEM images of the wrinkling patterns. (c) and (d) display one-dimensional straight buckles and herringbone patterns, respectively, with primary wavelength ~50 nm created using acceleration voltage of 5 keV and ion fluences 9.0×10^{13} and 5×10^{14} ions cm^{-2}, respectively. Bar = 400 nm. (e) Complex hierarchical patterns with primary wavelength ~465 nm created using an acceleration voltage of 30 keV and ion fluence 1.0×10^{16} ions cm^{-2}. Bar = 5 μm. (f) For an acceleration voltage of 30 keV and ion fluence 1.0×10^{17} ions cm^{-2}, complex wrinkling patterns and surface cracking were observed. Bar = 5 μm.

exposed to a focused ion beam of Ga^+ ions in a digital mode with multiple acceleration voltages (5, 10, 20 and 30 keV) and ion current in the range of 1 pA to 20 nA. The incident angle, defined as the angle between the incoming beam and the surface normal, was maintained at 0° and the beam dwell time was 3 μs in all cases. The SEM images in the exposed region were taken by a built-in secondary electron microscope.

The morphology of the wrinkling patterns created was examined using atomic force microscopy (Nanoscope III, Digital Instrument, NY) in the tapping mode measurement and SEM. The mapping between the morphology of the wrinkling patterns and acceleration voltage and ion fluence of FIB is shown in Figure 1b, while selected SEM figures of the induced patterns are depicted in Figure 1c–f. At each acceleration voltage, straight, one-dimensional buckles appear at low ion beam fluence, while at higher ion fluence more complex patterns develop, including herringbone and double-scale morphologies with two or more distinct wavelengths as seen in Figure 1b. The critical value of ion fluence associated with the onset of appearance of a given wrinkle pattern is higher at lower acceleration voltages. At very high fluence, complex patterns and cracking of the surface were observed, denoted by the 'surface cracking' in Figure 1b.

Figure 2a shows the average induced strain in the stiff skin as a function of FIB fluence for the acceleration voltages 10, 20 and 30 keV, respectively. The induced strain in the stiff skin induced by FIB irradiation was estimated by direct measurement of the surface length, L, along a trace across the surface. With L_0 as the straight-line distance between the ends of the trace, the strain approximation is taken as $(L - L_0)/L_0$. The average compressive strain in the stiff skin was calculated by averaging the strain along at least five traces for each morphology studied. The lowest ion fluence which causes appearance of one-dimensional straight buckles is in the order of 10^{13} ions cm^{-2} with a slight dependence on the acceleration voltage as shown in Figure 1b. The average induced strain at the onset of skin wrinkling is $\varepsilon_c \sim 3\%$ for the three sets of measurement shown in Figure 2a. Examination of the wrinkling patterns created by ion beams with acceleration voltages of 5 and 20 keV confirmed that the induced average strain in the skin at the onset of wrinkling formation is effectively independent of the ion beam acceleration voltage. The classical relationship for buckling of a linear elastic stiff skin with modulus, E_s, attached to a compliant substrate with elastic modulus, E_f, gives the critical strain associated with the onset of instability [2,3,25,26] as $\varepsilon_c \approx 0.52(E_s/E_f)^{2/3}$, independent of the skin thickness. Based on $\varepsilon_c \approx 3\%$, the modulus ratio is $E_f/E_s \approx 70$. The associated wavelength, λ_1, of the first wrinkles to form, referred to hereafter as the primary wrinkles, scales with the thickness of the stiff skin, t, according to $\lambda_1/t \cong 4(E_f/E_s)^{1/3}$.

The chemical composition of the region of the PDMS exposed to FIB for 10 and 30 keV (specifically, the concentration of three major chemical components of the PDMS, O, Si and C) was examined using Auger electron spectroscopy (Perkin Elmer 660, Perkin Elmer, MA) with a 2 keV electron beam and depth resolution of less than 2 nm. A depth profile for the chemical components was obtained using a controlled sputtering rate of 5.1 nm min^{-1}, calibrated by comparison to the sputtering rate of SiO_2 [27]. The results of this analysis are shown in Figure 2b for the substrate exposed to FIB with acceleration voltage of 10 and 30 keV and ion fluence of about 10^{13} ions cm^{-2}. In the region next to the surface the chemical composition is altered from

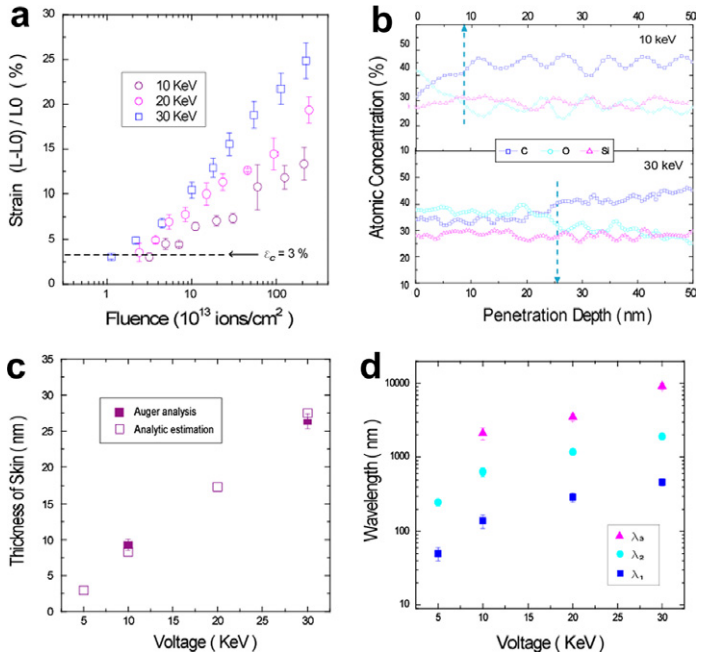

Figure 2. Quantification of the characteristics of wrinkling patterns induced by FIB. (a) Average compressive strain in the stiff skin formed on the surface area of the PDMS as a function of ion fluence for acceleration voltages of 10, 20 and 30 keV. The critical strain associated with the onset of wrinkles is ~3%. (b) Chemical composition of three major components (O, C and Si) of the PDMS substrate exposed to FIB with acceleration voltages of 10 and 30 keV as a function of depth below the surface. The surface layer affected by the irradiation is clearly evident, and the arrows indicate the skin thickness based on this analysis. (c) Estimates of the thickness of the stiff skin for wrinkling patterns created at acceleration voltages of 10 and 30 keV based on the Auger analysis. The analytical estimates of the skin thickness are based on buckling mechanics in combination with measured values of the critical strain and the primary wavelength of the wrinkles. (d) Wavelengths of the wrinkling patterns. The ion fluence influences the intensity of the wrinkles and their morphology (Fig. 1b), but it has little influence on the wavelength. For the lowest ion acceleration voltage, only hierarchical patterns with two wrinkling generations were created by increasing the ion beam up to 10^{16} ions cm^{-2}.

the PDMS substrate, taking a form somewhat similar to silica. By gauging the thickness of this altered region for the two acceleration voltages above, one arrives at the estimates of the thickness of the stiff skin in Figure 2c. The analytical thickness estimates in Figure 2c follow from using $E_f/E_s \approx 70$ and the measured primary wavelength, λ_1, in $t = \lambda_1/4(E_f/E_s)^{1/3}$. In the range of ion fluence considered, the skin thickness increases approximately linearly with the acceleration voltage from ~2.5 to ~28 nm.

Close examination of the undulations also shows that the wavelengths of the patterns depend primarily on the acceleration voltage. A critical ion fluence is required to produce a given pattern, but the fluence has little effect on the wavelength once the pattern has formed. These observations are consistent with the notion that the acceleration voltage sets the depth of penetration of the ions and therefore the thickness of the stiff skin, while the lateral strain induced by the FIB is controlled by the fluence. The three wavelengths plotted as a function of acceleration voltage in Figure 2d are measured within the hierarchal regime of Figure 1b. The finest wrinkling pattern has $\lambda_1 \approx 50$ nm and was created with an acceleration voltage of 5 keV (Fig. 1c), while the wrinkling patterns induced by an acceleration voltage of 30 keV have $\lambda_1 \approx 450$ nm. The largest measured wavelength is $\lambda_3 \approx 10$ μm for a hierarchical pattern induced by an acceleration voltage of 30 keV. Formation of hierarchical patterns, as well as evidence of their appearance in different skin–substrate systems, is discussed by Effimenko et al. [16] and Rizzeri et al. [26].

The wrinkling patterns in Figures 1 and 2 were created using a single scan mode. Additional sets of experiments involving multiple scanning modes were conducted to validate the conclusions asserted above. By subjecting the surface to multiple scans at the same acceleration voltage, we verified that the morphology of the wrinkling patterns is indeed controlled by the accumulative ion fluence, defined simply as the number of scans times the ion fluence per scan. By scanning the surface with the FIB at a low acceleration voltage and then rescanning at higher acceleration voltage, we saw that new undulations with longer wavelengths are superimposed on the primary set of wrinkles formed at the lower acceleration voltage.

A significant advantage of the surface modification offered by the technique discussed here is that wrinkles appear only on the areas of the PDMS exposed to the FIB. Areas covered by wrinkles can be selected by simply controlling the motion of the ion beam relative to the substrate [1]. In the present paper, the capabilities of this technique have been extended further by adopting the maskless patterning method of the FIB equipment. This method permits the accurate selection of the areas exposed to the FIB. Bitmap files of the exposure patterns, such as those shown in Figure 3, were imported as a virtual mask in the focused ion beam system. Surface areas (20 μm × 20 μm) of the PDMS substrate

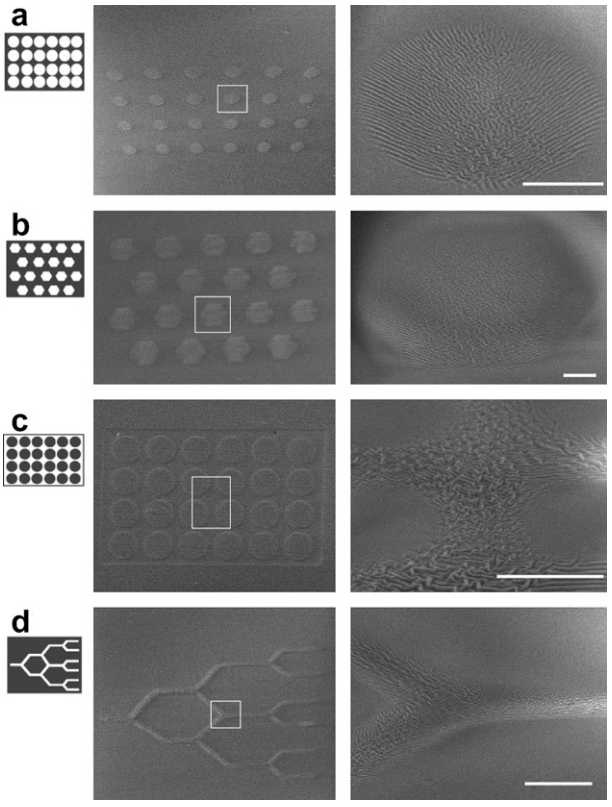

Figure 3. Selective patterning of the PDMS surface using maskless patterning. The bitmap files (shown on left for each pattern) were imported to the FIB such that only the white regions were exposed. Using a low energy ion beam of acceleration voltage 10 keV, wrinkling patterns with wavelength ~120 nm and amplitude of 5–30 nm were created on the exposed regions of the substrate. The ion fluence of the FIB within each patterned shape was 1.3×10^{15}, 2.1×10^{16}, 2.25×10^{15} and 2.3×10^{15} ions cm^{-2} for (a), (b), (c) and (d), respectively. The middle panels show the patterns, while the panels on the right are SEM figures of the wrinkles themselves over areas within the white rectangle. Bar = 5 μm.

were subject to FIB irradiation with acceleration voltage of 10 keV.

In conclusion, a promising method has been demonstrated for controlled creation of nanoscale wrinkling patterns on a polymeric surface using FIB. The wavelengths of the induced wrinkling patterns can be selected over a range of scales from tens of nanometers to microns by controlling the acceleration voltage, while the complexity of the wrinkle patterns is mainly influenced by the ion fluence. The proposed technique for controlled modification of polymeric surfaces has potential scientific and technological applications, such as building cell templates, microlenses and multi-functional microfluidic devices.

We thank Dr. M. Aziz for fruitful discussions. This work has been supported in part by the Korea Research Foundation under Grant M01-2005-000-10198-0 (M-W.M.), and the Center for Advanced Materials Processing (CAMP) of the 21st Century Frontier R&D Program (K.H.O.) and in part by the ONR under Grant N00014-04-1-0154 (M-W.M., J.W.H.) and the School of Engineering and Applied Sciences, Harvard University (A.V., J.W.H.).

[1] M.-W. Moon, S.H. Lee, J.-Y. Sun, K.H. Oh, A. Vaziri, J.W. Hutchinson, Proc. Natl Acad. Sci. USA 104 (2007) 1130.
[2] N. Bowden, S. Brittain, A.G. Evans, J.W. Hutchinson, G.M. Whitesides, Nature 393 (1998) 146.
[3] X. Chen, J.W. Hutchinson, ASME J. Appl. Mech. 71 (2004) 597.
[4] X. Chen, J.W. Hutchinson, Scripta Mater. 50 (2004) 797.
[5] R. Huang, J. Mech. Phys. Solids 53 (2005) 63.
[6] C.S. Chen, M. Mrksich, S. Huang, G.M. Whitesides, D.E. Ingber, Science 276 (1997) 1425.
[7] R. Jain, A.F. von Recum, J. Invest. Surg. 16 (2003) 263.
[8] X. Jiang, S. Takayama, X. Qian, E. Ostuni, H. Wu, N. Bowden, P. LeDuc, D.E. Ingber, G.M. Whitesides, Langmuir 18 (2002) 3273.
[9] M.T. Lam, S. Sim, X. Zhu, S. Takayama, Biomater. 27 (2006) 4340.
[10] A.K. Geim, S.V. Dubonos, I.V. Grigorieva, K.S. Novoselov, A.A. Zhukov, S.Y. Shapoval, Nature Mater. 2 (2003) 461.
[11] C. Harrison, C.M. Stafford, W. Zhang, A. Karim, Appl. Phys. Lett. 85 (2000) 4016.
[12] E.P. Chan, A.J. Crosby, Adv. Mater. 18 (2006) 3238.
[13] S.R. Kim, A.I. Teixeira, P.F. Nealey, A.E. Wendt, N.L. Abbott, Adv. Mater. 14 (2002) 1468.
[14] A. Khademhosseini, R. Langer, J. Borenstein, J. Vacanti, Proc. Natl Acad. Sci. USA 103 (2006) 2480.
[15] H.A. Stone, A.D. Stroock, A. Ajdari, Annu. Rev. Fluid Mech. 36 (2004) 381.
[16] K. Efimenko, M. Rackaitis, E. Manias, A. Vaziri, L. Mahadevan, J. Genzer, Nature Mater. 4 (2005) 1.
[17] J. El-Ali, P.K. Sorger, K.F. Jensen, Nature 442 (2006) 403.
[18] D.J. Beebe, J.S. Moore, Q. Yu, R.H. Liu, M.L. Kraft, B.-H. Jo, C. Devadoss, Proc. Natl Acad. Sci. USA 97 (2000) 13488.
[19] S. Klaumunzer, G. Schumacher, Phys. Rev. Lett. 51 (1983) 1987.
[20] E. Snoeks, T. Weber, A. Cacciato, A. Polman, J. Appl. Phys. 78 (1995) 4723.
[21] C.A. Volkert, J. Appl. Phys. 70 (1991) 1.
[22] K. Otani, X. Chen, J.W. Hutchinson, J.F. Chervinsky, M.J. Aziz, J. Appl. Phys. 100 (2006) 023535.
[23] T. van Dillen, E. van der Giessen, P.R. Onck, A. Polman, Phys. Rev. B 74 (2006) 132103.
[24] E.A. Wilder, S. Guo, S. Lin-Gibson, M.J. Fasolka, C.M. Stafford, Macromolecules 39 (2006) 4138.
[25] E. Cerda, L. Mahadevan, Nature 419 (2003) 579.
[26] R. Rizzieri, L. Mahadevan, A. Vaziri, A. Donald, Langmuir 22 (2006) 3622.
[27] S. Hofmann, Appl. Phys. 9 (1976) 59.